Microlens Fabrication by Selective Oxidation of Composition-Graded Digital Alloy AlGaAs

Ki Soo Chang, Young Min Song, and Yong Tak Lee

***Abstract*—We have fabricated refractive microlenses using selective oxidation of composition-graded digital alloy AlGaAs. The chirped short period superlattice of GaAs–AlAs was used to grade the composition of AlGaAs along the growth direction for a reproducible and controllable composition and oxidation profile. The oxidized profile of linearly composition-graded digital alloy AlGaAs shows a circular convex lens shape. The focused spot pattern of the beam at the focal point of the fabricated circular buried microlens reveals the strong focusing function of the microlens. Circular buried microlenses with mesa diameter of 20 μm exhibited focal length of 28–33 μm and a focused spot diameter of 4.0–6.4 μm, which are varied by oxidation time.**

***Index Terms*—AlGaAs, digital alloy, microlens, selective oxidation.**

I. Introduction

MICROLENSES and their arrays with diameters of a few to a few hundred micrometers are extensively used in optical systems and devices to increase the optical efficiency [1]. In particular, semiconductor microlenses that are directly formed on semiconductor material can have a large numerical aperture due to a large refractive index of semiconductor material that enables monolithic integration of active and passive optical component on the same chip, accompanying the possibility of simple and compact system packaging. In the free-space parallel optical link, as an example, the use of a microlens array integrated with vertical-cavity surface-emitting lasers (VCSELs) offers relaxed alignment tolerance, high optical beam quality, and lowered cost through a wafer-scale integration process [1]. Previously, various fabrication methods for a semiconductor microlens, such as photoresist reflow followed by dry etch [2], mass transport after preshaping [3], shadow mask regrowth [4], and diffusion-limited wet etching [5] were developed. However, those methods require multiple process steps for the fabrication of a microlens and the active alignment step for lens–laser monolithic integration.

In this letter, we propose and describe a new fabrication method of semiconductor microlenses using selective oxidation of composition-graded digital alloy AlGaAs. We also present the optical performance of fabricated microlenses. This method enables the self-aligned formation of a microlens on, or in, resonant cavity devices, such as a VCSEL.

Manuscript received August 1, 2005; revised September 27, 2005. This work was supported by MOST through the TND project.

The authors are with the Department of Information and Communications, Gwangju Institute of Science and Technology (GIST), Gwangju 500-712, Korea (e-mail: ytlee@gist.ac.kr).

Digital Object Identifier 10.1109/LPT.2005.860051

The native oxide converted from high aluminum content $Al_xGa_{1-x}As$ ($x > 0.85$) buried in GaAs–$Al_xGa_{1-x}As$ heterostructure can be formed in the way that the Al-containing layers are exposed in a water vapor ambient at elevated temperature [6]. Oxidized $Al_xGa_{1-x}As$ has properties, such as high selectivity for Al composition, electrical insulation, and a low refractive index, making it useful for electrical and optical confinement in a VCSEL [7]. Due to strong dependence of the oxidation rate on Al composition, we can obtain a desired oxidation profile (interface profile between oxidized and unoxidized AlGaAs) by properly grading Al composition of AlGaAs along the growth direction. In this way, we can form a buried refractive microlens.

II. Growth and Fabrication

We used a chirped short period superlattice of GaAs–AlAs to grade the composition of AlGaAs along the growth direction. The growth of composition-graded high-Al content analog alloy AlGaAs using molecular beam epitaxy (MBE) is achievable with change of cell temperature during growth, but the small Ga flux required to grow such structures may cause problems in the reproducibility and controllability of the composition and oxidation profile. Digital alloy, i.e., short period superlattices (SPSs) consisting of binary or ternary layers, have emerged as a solution for MBE growth of ternary or quaternary materials with versatile, accurate, and reproducible control of composition [8], [9]. In addition, digital alloys of a wide variety of compositions can be grown without additional source cells and without changing the effusion cell temperatures.

For a lateral oxidation of a thin $Al_xGa_{1-x}As$ layer, the oxidation rate dependence on a composition (x) of a digital alloy shows a similar trend with that of analog alloy, i.e., the oxidation rate of digital alloy $Al_xGa_{1-x}As$ drops by more than an order of magnitude for x decreasing from 1.0 to 0.9 [10]. However, the oxidation profile of a linear composition-graded bulk digital alloy shows a drastic difference from that of an analog alloy. In our experiment, the oxidation profile of linear composition-graded bulk analog alloy was concave in shape, whereas that of a digital alloy was convex. This can be attributed to the fact that there is a vertical oxidation as well as a lateral oxidation for bulk AlGaAs. For a composition-graded digital alloy AlGaAs consisting of GaAs–AlAs SPS, a thin GaAs layer acts as a vertical oxidation barrier, resulting in a convex lens-shaped oxidation profile. This makes the digital alloy suitable for the formation of a microlens using selective oxidation without a complex composition-grading scheme.

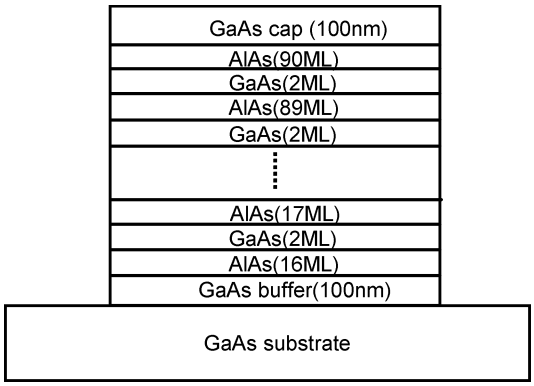

Fig. 1. Epitaxial layer structure of composition-graded digital alloy $Al_xGa_{1-x}As$ ($x = 0.89 \sim 0.98$) using chirped SPS of GaAs–AlAs.

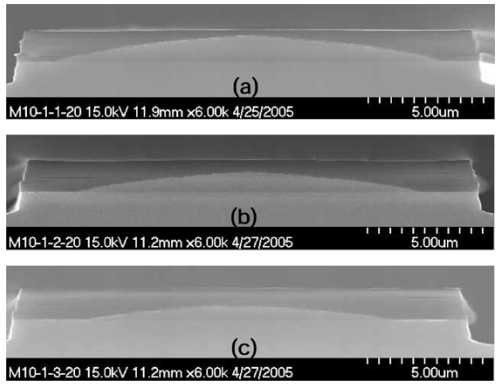

Fig. 2. Cross-sectional SEM images of 20-μm-wide stripe mesa after oxidation of composition-graded digital alloy $Al_xGa_{1-x}As$. Oxidation time: (a) 20, (b) 30, and (c) 45 min.

All the samples presented in this letter were grown using a DCA P600 solid source MBE system. Growth rates were calibrated using *in situ* optical reflectometry before every growth run. The calibrated growth rates of GaAs and AlAs were 2.0 and 1.48 Å/s, respectively.

To investigate the oxidation profile of a composition-graded digital alloy AlGaAs, we grew an epitaxial layer structure, as shown in Fig. 1. A 100-nm GaAs buffer layer was grown on the epiready GaAs (100) substrate followed by 1.27-μm digital alloy $Al_xGa_{1-x}As$, in which the average Al composition was graded from 0.89 to 0.98 along the growth direction. The chirped short period superlattice of GaAs–AlAs in 75 steps was used to grade the composition of AlGaAs. The structure was then capped with a 100-nm GaAs layer.

After the growth of the epitaxial layer, standard photolithography was used to pattern 20-μm-wide stripe mesas. The GaAs cap and AlGaAs layers were etched by $SiCl_4$–Ar plasma in an inductively coupled-plasma (ICP) etching system to expose the AlGaAs layer at the stripe mesa side wall for lateral oxidation. The etched samples were oxidized immediately after the etching process to avoid natural oxidation. Before each oxidation run, the oxidation furnace was allowed to equilibrate at an elevated temperature with water vapor supplied using nitrogen bubbled through a water bath kept at 90 °C. The flow rate of the nitrogen carrier gas was 2 *l*/min. The oxidations were carried out at a temperature of 400 °C for 20–45 min. After the oxidation, the samples were cleaved and the oxidation profiles were measured using a cross-sectional scanning electron microscope (SEM). Fig. 2 shows SEM images after oxidation for various oxidation times. The dark region is the oxidized AlGaAs, and the light region is the unoxidized AlGaAs and GaAs substrate. The oxidation profile shows a convex lens shape. For a detailed quantitative evaluation of an oxidation profile, we digitized the oxidation profile from the SEM image. Fig. 3 shows the digitized oxidation profile, which is shown to fit closely with a circle. The radius of curvature (ROC) estimated from the circular fit and the calculated focal length (FL) obtained using commercial ray tracing software are summarized in Table I. The refractive indexes of AlGaAs, Al-oxide, and GaAs used in simulation were 2.93, 1.6, and 3.38, respectively. Refractive index variation from bottom to top (<2%) in the composition-graded AlGaAs region was neglected in focal length calculation.

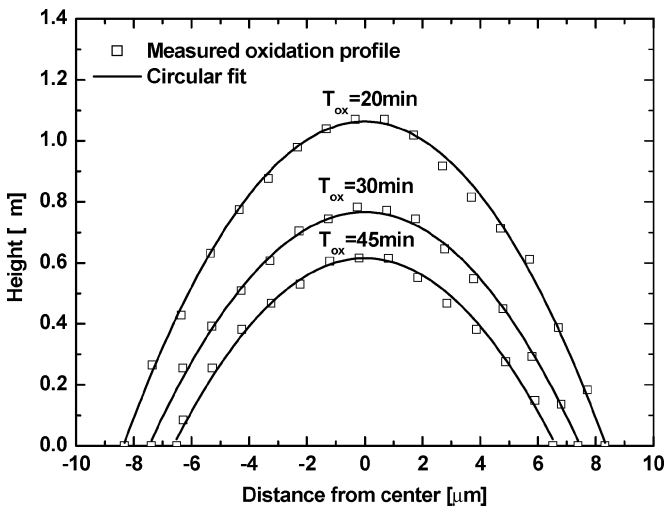

Fig. 3. Oxidation profiles of 20-μm-wide stripe mesa with circular fitting for various oxidation times (T_{ox}).

TABLE I
SUMMARY OF CHARACTERISTICS OF FABRICATED LENSES

Oxidation time [min]	Stripe mesa[a]		Circular mesa[b]	
	ROC [μm]	FL [μm]	FL [μm]	Spot size [μm]
20	33.4	27	28	4.0
30	36.8	29	31	5.4
45	37.5	30	33	6.4

[a] Stripe mesa width: 20μm

[b] Circular mesa diameter: 20μm,

For experimental confirmation of the proposed idea, we fabricated buried circular microlenses by selective oxidation. A both-side-polished GaAs substrate was used for transmission-type measurements of focal length and spot pattern. For a 20-μm-diameter circular mesa, oxidation was performed at 400 °C for 20–45 min, just as was done for the stripe mesa. We could not measure the oxidation profile of circular mesa due to the difficulty in the accurate cleaving along the center of the circular mesa.

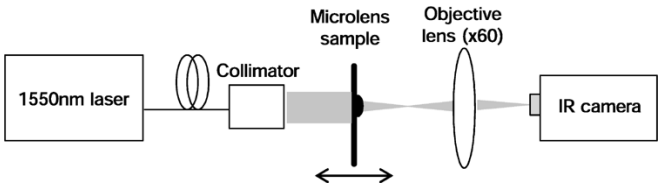

Fig. 4. Schematic diagram for focal length and focused spot pattern measurement.

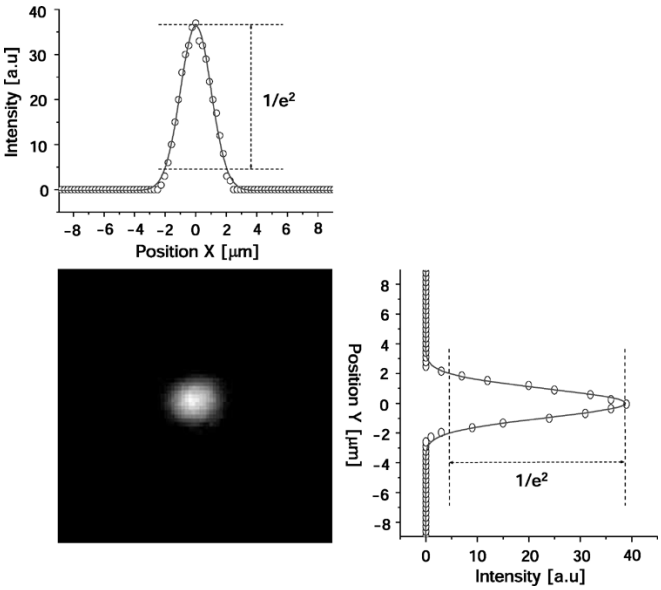

Fig. 5. Intensity distribution of laser beam at focal point of microlens (oxidation time: 20 min). Measured beam diameter of experimental intensity data (symbol) by Gaussian curve fitting (line) is 4.0 μm.

III. Optical Characterization

The optical properties of the fabricated circular microlenses were characterized by measuring the focal length and the two-dimensional focused spot pattern. A schematic diagram of the measurement setup is shown in Fig. 4. The setup consists of a 1550-nm laser coupled to a single-mode fiber pigtailed collimator, a $\times$ 60 microscope objective lens, IR camera, and image display and recording system. The fabricated microlens sample was mounted on a motorized translation stage, providing submicrometer minimum incremental motion so that the position of microlens could be controlled in a fine resolution. To measure the focal length of the microlens, first, the individual lens was set in a position where the microlens image was clearly seen by the IR camera; this denotes the zero position. Then, by moving the microlens toward the collimator along the optic axis, we noted the position at which the spot size was minimized. This moving distance is the focal length of the microlens under test. Fig. 5 shows the intensity profile of the beam at the focal point of 28 μm, which reveals the strong focusing function of the microlens and resembles that of a typical Gaussian beam with a diameter of 4.0 μm. For a 20-μm-diameter circular mesa with various oxidation times, the measured focal length and spot size are summarized in Table I. As the oxidation time increases, the focal length slightly increases due to the increase in ROC of the oxidation profile. For the same oxidation time, the focal length of the circular microlens is slightly longer than that of cylindrical microlens due to the faster oxidation rate of the circular mesa than the stripe mesa.

IV. Conclusion

We have fabricated microlenses by selective oxidation of a composition-graded digital alloy AlGaAs and characterized optical performances. The chirped SPS of GaAs–AlAs was used to grade the composition of AlGaAs. The digital alloy technique enables the growth of composition-graded high-Al content AlGaAs with a versatile, accurate, and reproducible control of composition and oxidation profile. Also, it enables the formation of microlenses using selective oxidation with simple linear composition grading. The cross-sectional SEM image, circular convex lens-shaped oxidation profile, and focusing test demonstrate that the fabricated microlenses have good optical properties. The most obvious advantage of fabricating microlenses using this method is that self-aligned microlens formation is possible on, or in, the optoelectronic devices, such as VCSELs, to improve device performance.

References

[1] H. P. Herzig, *Micro-Optics: Element, Systems and Application*. New York: Taylor and Francis, 1997.

[2] E. M. Strzelecka, D. A. Louderback, B. J. Thibeault, G. B. Thompson, K. Bertilsson, and L. A. Coldren, "Parallel free-space optical interconnect based on arrays of vertical-cavity lasers and detectors with monolithic microlenses," *Appl. Opt.*, vol. 37, pp. 2811–2822, 1998.

[3] E. M. Strzelecka, G. D. Robinson, L. A. Coldren, and E. L. Hu, "Fabrication of refractive microlenses in semiconductors by mask shape transfer in reactive ion etching," *Microelecton. Eng.*, vol. 35, pp. 385–388, 1997.

[4] Z. L. Liau, D. E. Mull, C. L. Dennis, R. C. Williamson, and R. G. Waarts, "Large-numerical-aperture microlens fabrication by one-step etching and mass-transport smoothing," *Appl. Phys. Lett.*, vol. 64, pp. 1484–1486, 1994.

[5] Y. -S. Kim, J. Kim, J. -S. Choe, Y. -G. Roh, H. Jeon, and J. C. Woo, "Semiconductor microlenses fabricated by one-step wet etching," *IEEE Photon. Technol. Lett.*, vol. 12, no. 4, pp. 507–509, Apr. 2000.

[6] K. D. Choquette *et al.*, "Advances in selective wet oxidation of AlGaAs alloys," *IEEE J. Sel. Topics Quantum Electron.*, vol. 3, no. 3, pp. 916–926, Jun. 1997.

[7] D. G. Deppe, D. L. Huffaker, J. Shin, and Q. Deng, "Very-low-threshold index-confined planar microcavity lasers," *IEEE Photon. Technol. Lett.*, vol. 7, no. 5, pp. 965–967, May 1995.

[8] J. D. Song, W. J. Choi, J. M. Kim, K. S. Chang, and Y. T. Lee, "MBE growth and optical properties of digital-alloy 1.55 μm multi-quantum wells," *J. Cryst. Growth*, vol. 270, pp. 295–300, 2004.

[9] G. W. Pickrell, J. H. Epple, K. L. Chang, K. C. Hsieh, and K. Y. Cheng, "Improvement of wet-oxidized $Al_xGa_{1-x}As$ ($x \sim 1$) thourgh the use of AlAs/GaAs digital alloys," *Appl. Phys. Lett.*, vol. 76, pp. 2544–2546, 2000.

[10] R. Todt, K. Dovidenko, A. Katsnelson, V. Tokranov, M. Yakimov, and S. Oktyabrsky, "Oxidation kinetics and microstructure of wet-oxidized MBE-grown short-period AlGaAs superlattices," in *Proc. Mater. Res. Soc. Symp.*, vol. 692, 2002, pp. 561–566.